



Distributed Temperature Profiling System Provides Spatially Dense Measurements and Insights about Permafrost Distribution in an Arctic Watershed

Emmanuel Léger¹, Baptiste Dafflon¹, Yves Robert¹, Craig Ulrich¹, John E. Peterson¹, Sébastien
5 Biraud¹, Vladimir E. Romanovsky², and Susan S. Hubbard¹

¹Lawrence Berkeley National Laboratory, Berkeley, CA, 94720, USA

²Geophysical Institute, University of Alaska Fairbanks, Fairbanks, 99775, USA

Correspondence to: Baptiste Dafflon (bdafflon@lbl.gov)

Abstract. Soil temperature has been recognized as a property that strongly influences a myriad of hydro-biogeochemical
10 processes, as well as containing important information on the properties modulating the soil thermal flux. In spite of its
importance, our ability to acquire soil temperature data with high spatial and temporal resolution and coverage is limited,
because of the high cost of equipment, the difficulties of deployment, and the complexities of data management. Here we
propose a new strategy that we call Distributed Temperature Profiling (DTP), which consists of cheap, low-impact, low-
power, vertically resolved temperature probes that independently and autonomously record soil temperature. We developed a
15 prototype DTP system for characterizing and monitoring near-surface thermal properties, using an unprecedented number of
laterally and vertically distributed temperature measurements. The DTP system was tested in an Arctic ecosystem near
Nome, AK, to identify near-surface permafrost distribution and various thermal regimes in a discontinuous permafrost
environment during the summer time. Results show that the DTP system enabled successful acquisition of vertically
resolved profiles of summer soil temperature over the top 0.8 m at numerous locations. DTP also enabled high resolution
20 identification and lateral delineation of near-surface permafrost locations from surrounding zones with no permafrost or deep
permafrost table locations overlain by a perennially thawed layer. The DTP strategy overcomes some of the limitations
associated with —and complements the strengths of— borehole-based soil temperature sensing as well as Fiber-Optic
Distributed Temperature Sensing (FO-DTS) approaches. Combining DTP data with co-located topographic and vegetation
maps obtained using Unmanned Aerial Vehicle (UAV) and Electrical Resistivity Tomography (ERT) data allowed us to
25 identify correspondences between surface and subsurface property distribution, and in particular between topography,
vegetation, shallow soil properties, and near-surface permafrost. Finally, the results highlight the considerable value of the
newly developed DTP strategy for investigating the significant variability and complexity of subsurface thermal and
hydrological regimes in discontinuous permafrost regions.



1 Introduction

Soil temperature and its spatial and temporal variability mediate a myriad of above- and belowground hydro-biogeochemical processes. Soil temperature is an important factor influencing the water and energy exchanges with the atmosphere, including evaporation (Smits et al., 2011). In addition, all chemical and biochemical reactions in soil, including those related to root and soil respiration and microbial decomposition, are temperature dependent (Davidson and Janssens, 2006). Thus, soil temperature plays an important role in plant growth and in soil carbon efflux and feedback on atmospheric CO₂ (Fang and Moncrieff, 2001).

Soil temperature influences many processes, but in turn it is controlled by climatic forcing and modulated by canopy characteristics, snow insulation, surface water, soil thermal parameters, and heat and water fluxes in the subsurface. Therefore, time-series of soil temperature can be used to estimate the influence of the above factors on the thermal regime. For example, time-series of temperature measurements can be used in a parameter estimation framework to quantify the thermal parameters and, potentially, the fraction of soil constituents including organic matter content (Nicolosky et al., 2009; Tran et al., 2017). Thermal temporal variability is also used to investigate fluid fluxes, surface water/groundwater exchange, and groundwater recharge (Briggs et al., 2012; Stonestrom and Constantz, 2003).

The significant spatial and temporal variability in the aforementioned processes require surveying and/or monitoring multiple locations to capture and understand the heterogeneity of the studied system. Conventional point-sensor methods for characterizing and monitoring temperature predominantly rely on measurements collected using point sensors placed directly in the ground, or deployed as a string of sensors along a probe or a borehole. Different types of sensors are commonly used, including thermistors, thermocouples, and temperature-sensing integrated circuits. Usually, a data logger is physically connected to multiple thermal sensors, although a growing number of studies use self-recording sensors that collect and store the data individually (including iButtons, Onset Pendants, LogTag) (Hubbart et al., 2005; Lundquist and Lott, 2008) to increase the number of spatially distributed temperature measurements at a reasonable cost. Fiber-Optic Distributed Temperature Sensing (FO-DTS) offers an alternative to point-sensor methods in studies where temperature measurements with high spatial and temporal-sampling resolution are needed (Tyler et al., 2009). The optimal sensing approach is case specific and depends on many factors and requirements, including material cost, deployment and management cost, spatial and temporal resolution and coverage, data resolution, and data accuracy (e.g., Lundquist and Lott, 2008).

While the cost per traditional temperature point sensor can be considered low (in the range of \$1 to \$150), the total cost using the point-sensor method—including data logger, packaging, installation, localization and management—make this method often expensive to install in large numbers. Several studies have focused on evaluating various approaches to decrease the cost and increase the number of measurement locations. The best example of this was the deployment of ~1600 self-recording temperature sensors (TRIX-16 Logtag sensors) across a domain extending from the Boise Basin, Idaho, to southern British Columbia, to evaluate downscaling of air temperature from long-term weather stations—using covariates that had established physical links to surface air temperature, including solar insolation, soil moisture, local topography,



canopy cover, geopotential height, and humidity (Holden et al., 2016). In another study, 390 self-recording temperature sensors (iButtons) were deployed to record the distribution of ground-surface temperature in a region with high topographic variability in the Swiss Alps. The acquired data were used to document the effect of elevation, slope, aspect and ground cover type on the mean annual ground-surface temperature (Gubler et al., 2011). Similarly, 171 sensors (mostly iButtons) recording the distribution of ground surface temperatures across a climatic gradient from continuous to sporadic permafrost in Norway documented the pronounced control of snow depth on the local-scale variability of mean annual ground-surface temperature (Gisnås et al., 2014). While networks of low-cost distributed temperature sensors have concentrated primarily on air temperature measurements (Holden et al., 2016; Hubbard et al., 2005; Whiteman et al., 2000) and ground-surface temperature (Davesne et al., 2017; Gisnås et al., 2014; Gubler et al., 2011; Lewkowicz et al., 2012; Lundquist and Lott, 2008), little effort has been made to increase vertical- and lateral-direction measurements in soil. Thus, the installation of sensor networks for soil temperature is typically too spatially sparse to identify local-scale vertical and lateral variations in soil thermal regimes. Such variations are relevant for optimally quantifying, (among other effects) the influence of soil-snow-inundation-topographic-vegetation properties on the subsurface thermal regime, the fraction of soil constituents at numerous locations, and the role of subsurface hydrology and advective heat transport in permafrost distribution and evolution.

Note that while the development of Fiber-Optic Distributed Temperature Sensing (FO-DTS) has offered some promise in providing soil temperature measurements with high spatial and temporal-sampling resolution, this approach is limited to specific applications and requires significant initial investment (>\$30K, Lundquist and Lott, 2008), as well as careful experimental design to produce to its capacity (Lundquist and Lott, 2008; Tyler et al., 2009). In particular, FO-DTS deployment can require a dynamic calibration (Hausner et al., 2011), the occasional need of a fusion splicer to join fibers in the field, the disturbance of the investigated environment by the creation of a trench or a crack while installing and removing the cable, and the risk of losing a large amount of data in case of instrument, cable or power failure. FO-DTS is primarily well suited where these issues can be easily addressed, such as for applications in a streambed, at the ground surface, in wells, in trenches, and in artificial ecosystems (Briggs et al., 2012).

Quantifying soil temperature has shown to be particularly important for understanding the evolution of Arctic permafrost regimes (e.g., Brewer, 1958; Jorgenson et al., 2010; Lachenbruch and Marshall, 1969). Brewer (1958) recognized the dramatic influence of surface hydrology on permafrost thawing by using thermistor strings (Swartz, 1954), which monitored temperature in a lake down to depths of a few tens of meters below the lake bottom near Barrow, AK, over the course of a year. Lachenbruch and Marshall (1969) subsequently studied the effect of latent heat on permafrost temperature near shorelines and lakes where thermal profile anomalies were observed. In the 1980s, several studies focused on Arctic permafrost, including its relationship to historical temperature and climate change trends (Osterkamp, 1987, 1983, 1985; Osterkamp and Gosink, 1991). Osterkamp (1985) improved permafrost temperature measurements by developing a long thermistor cable that could sense temperature with high precision at its end. Many studies investigated further permafrost thermal hydrology and long-term temperature variations (e.g., Biskaborn et al., 2015; Burn, 2002; Osterkamp, 1987;



Romanovsky and Osterkamp, 2000). Besides the use of point sensors for temperature measurements, FO-DTS has been applied in a few cases, including monitoring permafrost temperature along a transportation infrastructure (Roger et al., 2015) and detecting permafrost degradation during a controlled warming experiment (Wagner et al., 2018). In both cases, possible long-term disturbance resulting from the FO-DTS installation was not addressed, because the installation was made in the context of infrastructure improvement in the first case and short-term experiment in the second case.

Studies conducted over the last six decades in the Arctic have led to a steady improvement in our ability to evaluate permafrost distribution and characteristics, as well as our ability to evaluate the complex influence of various soil, vegetation, and atmosphere factors. These factors include snow cover (Stieglitz et al., 2003; Zhang, 2005), air temperature (Zhang et al., 1996), vegetative layers (Sturm et al., 2001), soil thermal parameters (Romanovsky and Osterkamp, 1995; Tran et al., 2017), soil hydrological properties (Dafflon et al., 2017), CO₂ and methane fluxes (Wainwright et al., 2015), and geomorphology (Jorgenson et al., 2010; Rowland et al., 2011). At local scales, studies have also shown the complexity of the system and the value of integrating multiple approaches, including soil sampling, point sensor methods, geophysical techniques, and remote sensing (Dafflon et al., 2016; Hubbard et al., 2013).

Despite many advances in improving our understanding of the Arctic Ecosystem, the acquisition of spatially and temporally dense soil temperature measurements over relevant spatial scales is critically important for advancing the predictive understanding of natural and managed ecosystems, yet is still challenging. Improving our predictive understanding of the interaction between plant distribution/dynamic and subsurface thermal and hydro-biogeochemical processes requires spatially and temporally dense measurements that yield important information about the energy and water fluxes in the subsurface. Indeed, the energy exchange between the atmosphere and soil minerals is strongly mediated by snow, surface water, vegetation, and organic layers (Cable et al., 2016; Jorgenson et al., 2010), with each of these factors being highly spatially and temporally variable. Although this complexity has been recognized, the ability to quantify each of these processes and how they influence soil thermal and hydro-biogeochemical processes over time is still limited. Improving our ability to quantify how the lateral and vertical heterogeneity of processes are related is necessary, both to advance our mechanistic understanding, and to develop multiscale sensing and modeling strategies that better simulate hydro-biogeochemical processes and ecosystem evolution in a changing climate.

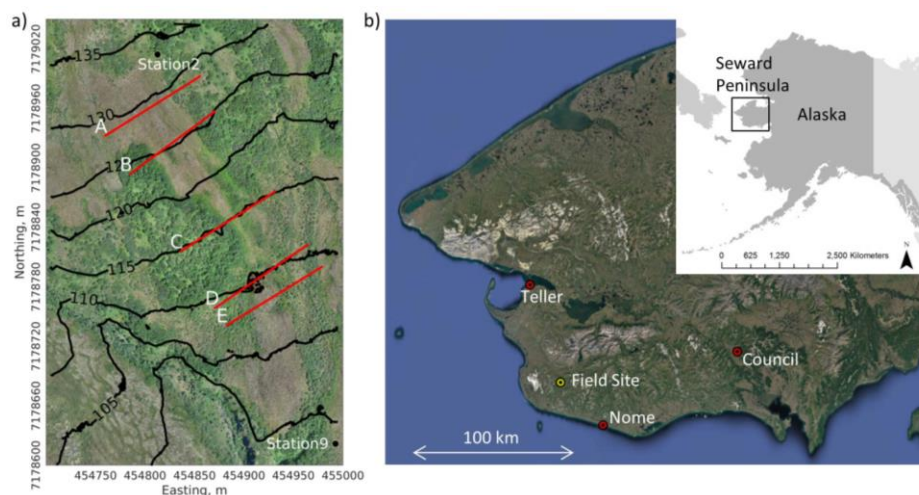
In this study, we introduce a novel sensing strategy that we call Distributed Temperature Profiling (DTP)—a strategy for obtaining spatially and temporally dense soil temperature measurements at flexible spatial scales—and then we test this strategy in an Arctic ecosystem. To this end, we built a prototype DTP system that consists of low-cost, low-impact, low-power-consumption, independent, vertically resolved temperature probes. *Low-cost* is defined here as being possibly built at a cost of less than \$100 per probe and logger, not requiring any annual fee, and deployable at hundreds to thousands of locations. This approach fully explores the development of inexpensive, nimble, and low-powered single-board computers coupled with the large variety of sensors available owing to the development of the “Internet of Things” (Ashton, 2009) and “Makers Movements” (Dougherty, 2012). The DTP prototype provides measurements over the first meter below ground surface at numerous locations at low cost and with rapid survey time. We tested the DTP strategy over more than one



hundred locations on July 17, 2017—with repeated measurements at 40 locations on September 20, 2017— within a 125 x 350 m² area in a discontinuous permafrost sub-Arctic environment, to investigate the local distribution of near-surface permafrost and its link with surface properties. We further compared DTP measurements with Electrical Resistivity Tomography (ERT) and Unmanned Aerial Vehicle (UAV) data collected at the site around July 17, 2017, to document the value of the DTP measurements for interpreting permafrost variability and possible controls.

2 Site Description

We performed our study in a watershed about 40 km northwest of Nome, AK, specifically along Teller Road, as part of the Next Generation Ecosystem Experiment project (NGEE-Arctic) (Figure 1). This “Teller watershed” can be considered to be representative of discontinuous permafrost systems, based on our preliminary investigations at the site, a numerical study evaluating the role of preferential snow accumulation in through Talik development under similar meteorological forcing (Jafarov et al., 2018) and other studies performed on the South Seward Peninsula (e.g., Yoshikawa and Hinzman, 2003). This study is the first (to our knowledge) to evaluate the permafrost distribution and co-variability with surface properties at this site. The watershed is characterized by a 130 m elevation gradient, the presence of solifluction lobes, a stream with a few confluents, and diverse vegetation cover—including tall shrub, dwarf shrub, moss, and graminoids (Figure 1). The National Ocean and Atmospheric Administration’s (NOAA’s) meteorological station at Nome Municipal Airport indicates that over a five-year average (2013 to 2017) the mean annual air temperature is -1.02°C, the yearly cumulative rain precipitation is 450.6 mm, and the yearly cumulative snow fall is 1704.8 mm. At the Teller watershed, the snow depth varies significantly from about 0.2 to 2 m, depending on the location and the year. The main DTP survey was conducted along five 120 m long transects within a 125 x 350 m² study area (Figure 1) on July 17, 2017, during a period expected to be near or at the peak of the vegetation growing season. During that campaign, sparse measurements collected with a 1 m tile probe indicated that the thawed layer was 0.4-0.6 m thick at a few locations. (Note that at most locations, the tile probe measurements were unsuccessful because of the absence of permafrost in the top 1 m and/or the presence of rocky soil.) A second short campaign, in which only DTP data were acquired along two of the five transects, took place on September 20, 2017 at the end of the summer season.



5 **Figure 1:** a) Aerial view of the investigated site in the Teller watershed, which includes a hillslope and a flatter toe area. Tall shrubs are dark green, mosses are bright green, and graminoids and dwarf-shrub dominated areas are light brown. The RGB-mosaic is overlain with the location of the two long-term monitoring stations in this area, the location of transects surveyed in this study, and topographic isolines (in meter amsl.). b) Location of the investigated field site on the South Seward Peninsula in Alaska.

3 Materials and Methods

3.1 Distributed Temperature Profiling Strategy

The fundamental concept behind the DTP system involves using a network of vertically resolved temperature probes and accompanying loggers that provide temperature at multiple depths and locations, and enables deployment over tens to thousands of locations because of its low cost and automated data management. Note that such a system can be deployed both as a characterization tool or for monitoring purposes. A DTP prototype system involving 30 probes was designed and built at the Lawrence Berkeley National Laboratory. While the number of probes is still rather small, to our knowledge this is the first time that such a vertically and laterally dense network of temperature measurements has been realized.

Each probe included 11 digital thermometers located 8 cm apart in the vertical direction. Each sensor was soldered on a thin copper sheet, inserted in a 9.5 mm outside-diameter PVC tube, and thermally isolated from other digital thermometers on the probe by epoxy-based glue. The digital thermometers used were the DS18B20 (Maxim Integrated™), which were 12 bits corresponding to a resolution of 0.0625°C and sold by the manufacturer as ±0.5°C accurate (<https://datasheets.maximintegrated.com/en/ds/DS18B20.pdf>). Data logging was performed individually for each probe across the network using a coupled Raspberry-Pi 3 single-board computer and a PYTHON-based acquisition protocol. The material involved in the construction of each probe with its coupled logger cost ~US \$90 (including the Raspberry). The probe sleeve and filling material were partly influenced by the work of Bill Cable, who built probes with vertically placed, highly accurate analog thermistors (led by Bill Cable, UAF, AK, <http://permafrost.gi.alaska.edu/content/thermistor-probe-construction>). While Cable's work was relevant for obtaining high vertical resolution at specific monitoring locations, here



we concentrated on building a much-lower-cost probe, integrated with a logger system and highly duplicable. Importantly, the prototype described here was intended for testing an acquisition strategy, and in no way represented the ideal DTP system with regard to hardware and software. Based on the results of this study, research is in progress to develop a DTP system with an extraordinarily low production and assembly cost; miniaturized data-logger; automated data acquisition, management, and transfer; and open source software and hardware to encourage community-based development and deployment.

The DTP prototype system was deployed sequentially at several locations in the Teller watershed. A tile probe with the same diameter as the temperature probe was first used to create a hole in the soil, wherein the temperature probe was then inserted while still being in tight contact with soil. The probes were inserted into the ground every 5 m along each transect, and left in place for data acquisition for ~30 minutes to ensure thermal equilibrium with the soil temperature. They were then moved to the next position. Thirty minutes to ensure thermal equilibrium was defined as a safe choice, based on preliminary tests that showed that 20 minutes were needed to approach a constant temperature in a $\pm 0.1^\circ\text{C}$ range. Also, the influence of time of day at which data acquisition occurred was evaluated using two of the probes that monitored diurnal soil temperature variations. This dataset showed that only the shallowest temperature sensors (\approx top 25 cm of soil) were affected by diurnal variations during the July campaign at the Teller site. Further, the DTP measurements presented here did not get corrected with any in-house calibration factors. Preliminary tests showed that the accuracy was better than the $\pm 0.5^\circ\text{C}$ accuracy (which we interpreted as three standard deviations) claimed by the manufacturer. Because of the length of the probe and the difficulty of maintaining a large volume of ice and/or water at constant temperature over space, no sensor-specific calibration curve could be easily defined while ensuring that it would increase sensor accuracy significantly. Finally, the only applied processing on the temperature data was for extracting temperature at 0.8 m depth. To ensure the comparison of soil temperature at that depth at various locations, we conducted a linear fit of the three deepest measurements along the probe. Extrapolation of temperature to 0.8 m depth occurred only at a few locations where the probes could not be pushed down to 0.8 m depth, due to the presence of permafrost or rock.

3.2 Point-scale Measurements, Including Temperature at Monitoring Stations

All measurement locations and elevations were surveyed with a Real-Time Kinematic (RTK) GPS, with centimeter accuracy in latitude/longitude positioning and elevation. Average soil water content in the upper 30 cm of soil was estimated at each DTP probe location along the transects using a Time Domain Reflectometry (TDR) probe (6050X1 TRASE System I portable unit) with 30 cm metallic probes. In addition to the DTP data, soil temperature data were also obtained from long-term conventional thermal monitoring stations established in the Teller watershed, each of which included five conventional temperature sensors and data loggers (Onset, Cape Cod, Massachusetts). The reported accuracy of these temperature sensors is 0.25°C ; however, an ice bath calibration was performed prior to installation, improving the accuracy for temperatures near 0°C to approximately 0.03°C (Cable et al., 2016). Each of these conventional temperature sensors was attached to a thin



PVC tube buried at different depths, ranging from 0.02 to 1.5 m below ground surface. Monitoring Stations 2 and 9, which were close to the investigated zone, were used to evaluate year-round temporal changes in temperature.

3.3 Electrical Resistivity Tomography

Electrical Resistivity Tomography data are typically collected using electrodes inserted into the ground, where the current is injected between two electrodes and the electrical potential difference is determined between two others (Binley and Kemna, 2005). The acquired resistance dataset is then inverted to estimate the spatial distribution of soil electrical resistivity (Rücker et al., 2017). The electrical conductivity (or its inverse, electrical resistivity) response is influenced by subsurface properties such as water/ice content, fluid electrical conductivity, lithological properties such as clay content, and soil temperature (Schön, 2015). ERT is increasingly used to identify permafrost distribution and characteristics, and to complement other measurements, including soil temperature (e.g., Dafflon et al., 2016; Léger et al., 2017; Minsley et al., 2012). In this study, ERT was used to complement DTP data, and in particular the assessment of the potential links between what is observed in the top meter of soil and the deeper subsurface heterogeneity in physical and hydrothermal properties. Given that advanced analysis and interpretation of ERT data is beyond the scope of this study, here we qualitatively compared DTP and ERT signatures and discuss their joint value for inferring the presence of near-surface permafrost.

The electrical resistivity surveys were carried out using a MPT DAS-1 system with a 120-electrode structure and one-meter spacing. The data were acquired in the frequency domain using dipole-dipole geometry. ERT data were inverted using the Boundless Electrical Resistivity Tomography (BERT) code (Rücker et al., 2006; Rücker et al., 2017; Rücker and Spitzer, 2006), which is a finite-element-based inversion process. No temperature correction was applied to the inverted ERT data, because of the large range of resistivity values observed compared to the effect of temperature on the data, and because of the unavailability of spatially distributed temperature measurements deeper than 0.8 m depth.

Based on permafrost resistivity ranges associated with field datasets (e.g., Dafflon et al., 2016; Hilbich et al., 2008; Krautblatter et al., 2010; Marescot et al., 2008) and laboratory datasets (Hauck, 2002; Wu et al., 2013), and assuming low salinity and low clay content at the investigated site, we postulated that high resistivity values from 1000 to 7000 Ohm.m were primarily related to the presence of permafrost when encountered close to the surface (in the top 4 meters). Those high values may also be related to the presence of bedrock or permafrost if encountered deeper below the surface. Based on Dafflon et al. (2017) at another Arctic site, resistivity values below 400 Ohm.m were interpreted to correspond to unfrozen conditions, while values between about 400 and 1000 Ohm.m were interpreted to correspond to frozen, partially frozen, or unfrozen conditions.

3.4 Unmanned Aerial Vehicle

UAV-based optical imagery was collected to reconstruct a color orthomosaic and Digital Surface Model (DSM) in order to understand vegetation distribution and topographic trends. UAV-based imaging was performed during the July 2017 campaign using a 3DR Solo UAV and a Sony 5100 as a sensor. The orthomosaic and DSM reconstructions (Figure 1) were



inferred using a commercial software (PhotoScan from Agisoft LLC) and georeferenced using targets set on the ground and measured with a RTK GPS. The final resolution and uncertainty of the DSM and color orthomosaic were about 4 cm in x,y,z directions. (More details on UAV-based imaging can be found in Dafflon et al. (2016)). To estimate a digital terrain model (DTM) proxy from the DSM, we re-interpolated the elevation after removing pixels showing a difference greater than 0.5 m
5 between their elevation and the minimum elevation in a centered 10x10 m² window. This enabled us to partially remove the presence of shrubs, while the obtained DTM proxy involves variable spatial resolution that is always lower than the original DSM.

4 Results

In this section, we present the DTP dataset along with other independent and more commonly acquired datasets bearing
10 information on the subsurface thermal regime. An evaluation and discussion of the value of the DTP dataset, and of how such a dataset can successfully complement other independent datasets, will be provided in Section 5.

Figure 2 shows the soil temperature at 0.8 m depth on July 17 obtained from the DTP system overlain on the reconstructed color orthomosaic. For enabling the comparison of data at similar depth, temperature values from locations where the probe could not be pushed entirely into the ground have been extrapolated to 0.8 m depth, which is the case for the
15 five locations showing the coldest temperatures along Transect E (Figure 2). The DTP dataset shows that the lateral variability in soil temperature at 0.8 m depth is very low over some distance intervals but very abruptly varying in several other locations, with changes of up to 6°C occurring over a 5 m distance or less (Figure 2). Most abrupt lateral changes in temperature at 0.8 m depth occur at 15 and 75 m along transect A, at 40 and 75 m along transect B, and at 35 and 65 m along transect E.

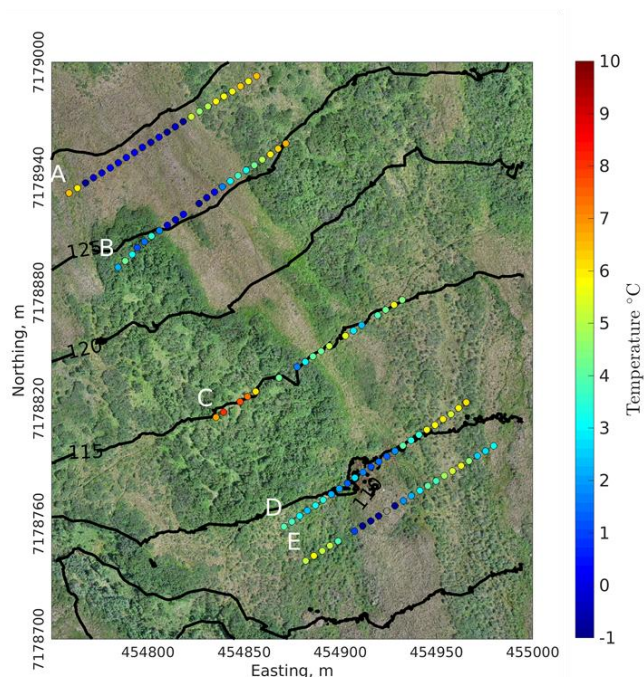
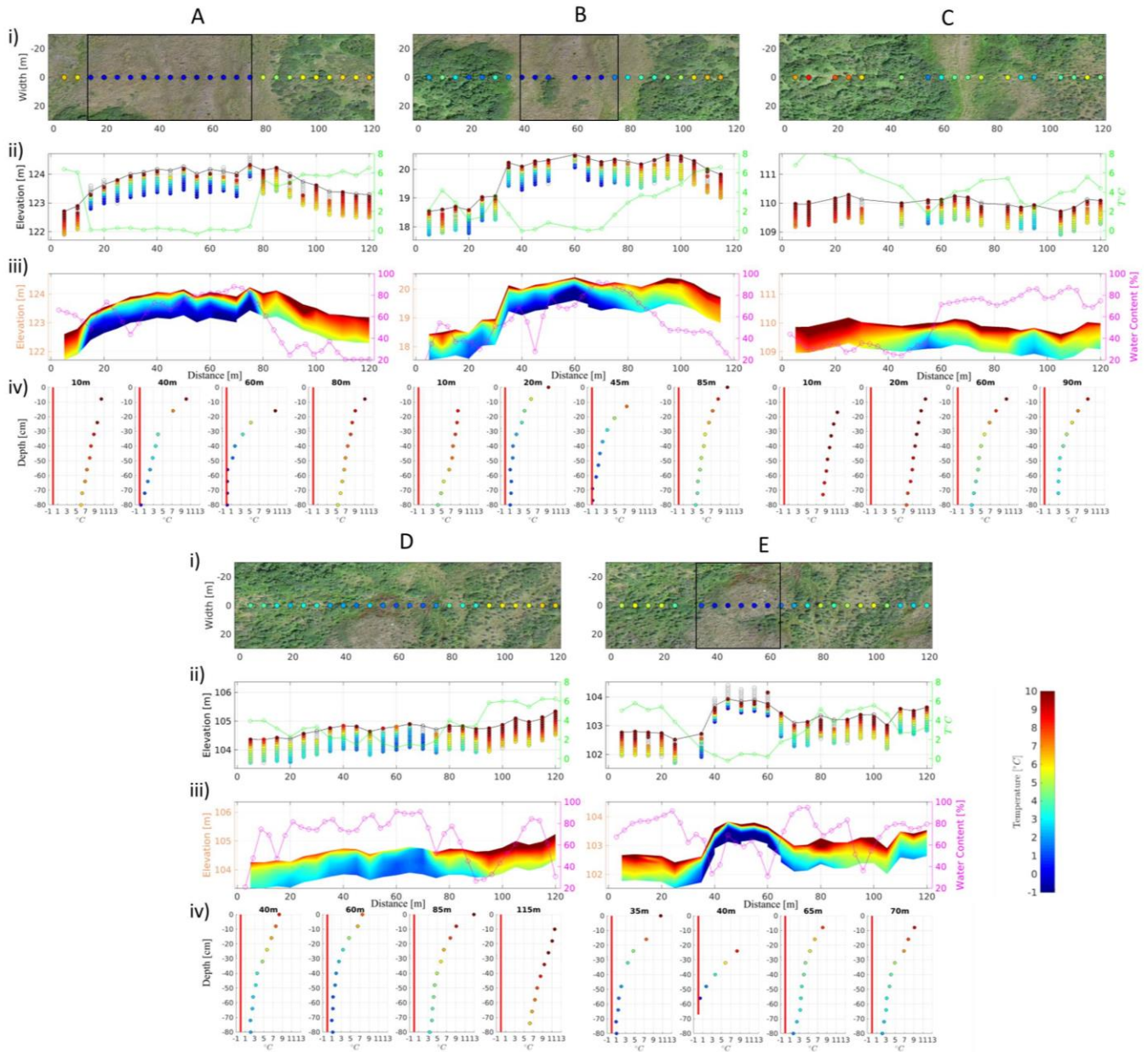


Figure 2: Temperatures at 0.8 m depth extracted from the DTP dataset collected on July 17 and overlain on Figure 1.

Figure 3 shows each transect in a relative coordinate system, in order to accommodate visualizing topography, vegetation type, soil moisture, and the July 17 vertically resolved DTP data together. Based on vertically resolved DTP data, soil temperature close to or below 0°C at 0.8 m depth (with a trend in temperature with depth going clearly toward negative temperature values) indicates the presence of near-surface permafrost. This is the case between 15 and 75 m along transect A, 40 and 75 m along transect B, and 35 and 65 m along transect E. The shallowest thaw layer (0.45 m) is observed at 45 m along transect E. This location also corresponds to the lowest temperature at 0.8 m depth, once we extrapolate soil temperature to this depth. The vertical thermal gradient in the top 0.8 m of soil, and the measurements of water content in the top 0.3 m using a TDR, show sharp changes at a similar location, while their values are not always positively correlated (Figure 3). Locations identified as near-surface permafrost along transects A and B show high soil water content in the top 0.3 m, while a location identified as near-surface permafrost along transect E shows low water content in the top 0.3 m.



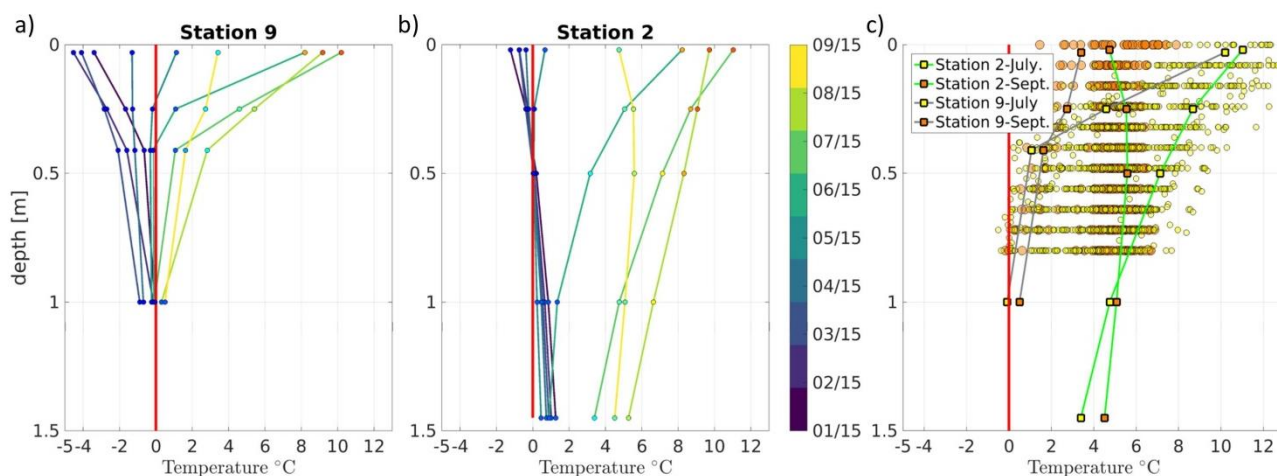
5 **Figure 3: DTP data collected on July 17, 2017, along A-E transects. (i) Aerial view of the A-E transects in relative coordinate systems, overlain by temperature at 0.8 m depth and consequently identified shallow permafrost areas (black rectangles), (ii) DTP temperature profiles and DTP temperature at 0.8 m depth, (iii) Interpolated temperature map of the first 0.8 meter with topography and surface water content obtained from TDR, and (iv) temperature profiles at selected locations along the transects.**

These abrupt lateral changes in soil temperature also correspond to changes in vegetation and topography (Figure 2 and 3). Figures 2 and 3 suggest that in general the soil temperatures at 0.8 m depth are the highest under tall-shrub-covered areas (up to 7.5°C), and the lowest under graminoids and dwarf-shrub-dominated areas (down to 0.2°C or below). This general



5 trend is modulated by or intertwined with many factors. The topographic lows along each transect tend to correspond to warmer soil temperatures at 0.8 m depths than the topographic highs. Given that the transects are oriented quite perpendicularly to the general slope aspect (Figure 2), topographic lows correspond here to preferential drainage paths crossing the transects perpendicularly and possibly related to ground erosion and/or ground settlement, as well as to locations with higher accumulation of snow during the winter.

In Figure 4, the soil temperature data are compared to the two long-term thermal monitoring stations (Figure 1) to evaluate any potential limitations in interpreting the one-time DTP dataset, and to evaluate the value of acquiring spatially dense DTP data. Note that while the DTP system can be deployed for monitoring purposes, here we concentrated on first evaluating its value by acquiring an initial large dataset in July 2017 and later repeating measurements along transects B and C in September 2017. Figures 4a and 4b show the soil vertical profile of temperature from the long-term monitoring stations measured every mid-month (i.e., every 15th day of the month) from January to September 2017. Figure 4c shows the soil vertical profile of temperature from the long-term monitoring stations overlain on the distribution of DTP data at many other locations for each depth, in July and September. Soil temperatures at Station 9 are colder than at Station 2 all year around, with a few exceptions for the shallowest measurement. Soil temperature data at Station 2 and 9 are in the upper and lower range of temperature values observed using the DTP system, respectively. Several locations in the DTP dataset show warmer or colder temperatures and represent end members in the system.



20 **Figure 4: Temperature profile at Station (a) 9 and (b) 2 at every mid-month from January 15, 2017 to September 15, 2017. The zero Celsius degree line is in bright red. (c) Comparison of temperature measurements at Stations 2 and 9 (solid lines) with DTP measurements (circles) along transects A to E on July 17 (yellow) and along transects B and C on September 20 (orange).**

Based on the monthly vertical profiles of temperature at Station 2 and in particular their vertical gradient, if present, the permafrost at this location is much deeper than 1.5 m (Figure 4). Note that in this case the surficial seasonally frozen layer that developed during the freezing season has entirely thawed before June 15. This observation confirms that the DTP dataset on July 17 is not threatened by potential misinterpretation of near-surface permafrost that could occur if a seasonally



frozen layer over perennially unfrozen soil were present. Station 9 corresponds to a location potentially having near-surface permafrost, with an active layer freezing entirely during the freezing season. Further, Stations 2 and 9 both show that the vertical profile of temperature has a sharp gradient in the top 0.25 to 0.5 m depth, while at greater depth the temperature has an increasingly asymptotic behavior. This expected behavior (based on the physics of thermal flux) underlines the importance of measuring temperature with highest vertical resolution close to the surface, while still acquiring measurements deeper than 0.5 m where asymptotic trends in soil temperature with depth are more present and strongly informative on the deeper thermal regime.

In Figure 5, the DTP dataset collected along transects B and C on September 20 is displayed in a similar way to the DTP dataset collected on July 17 in Figure 3. Figure 5iv shows four of the DTP vertical profiles of soil temperature acquired on September 20 and the corresponding ones collected on July 17. The DTP soil temperature at 0.8 m depth measured on September 20 shows a very similar spatial trend (although with different absolute values) to that measured on July 17, with clearly identifiable near-surface permafrost locations (Figure 5i and Figure 3i). The air temperature in September is colder than in July, and thus the top 15 cm of soil or more (depending on the location) are colder on September 20 than on July 17. Compared to July 17 DTP data, the DTP vertical profiles on September 20 show lower thermal gradients, as expected at the end of the summer season. The majority of locations show warmer soil temperature in the 0.5 to 0.8 meter depth interval on September 20 than on July 17, while other locations already show the effect of the decrease in downward heat flux at the end of the summer in this interval. The spatiotemporal difference in DTP vertical profiles between September 20 and July 17, and between the various locations, underlines the complexity of how the heat flux is mediated by soil thermal characteristics in the investigated depth interval, as well as by surface and vegetation properties and the thermal regime at deeper depth than 0.8 m.

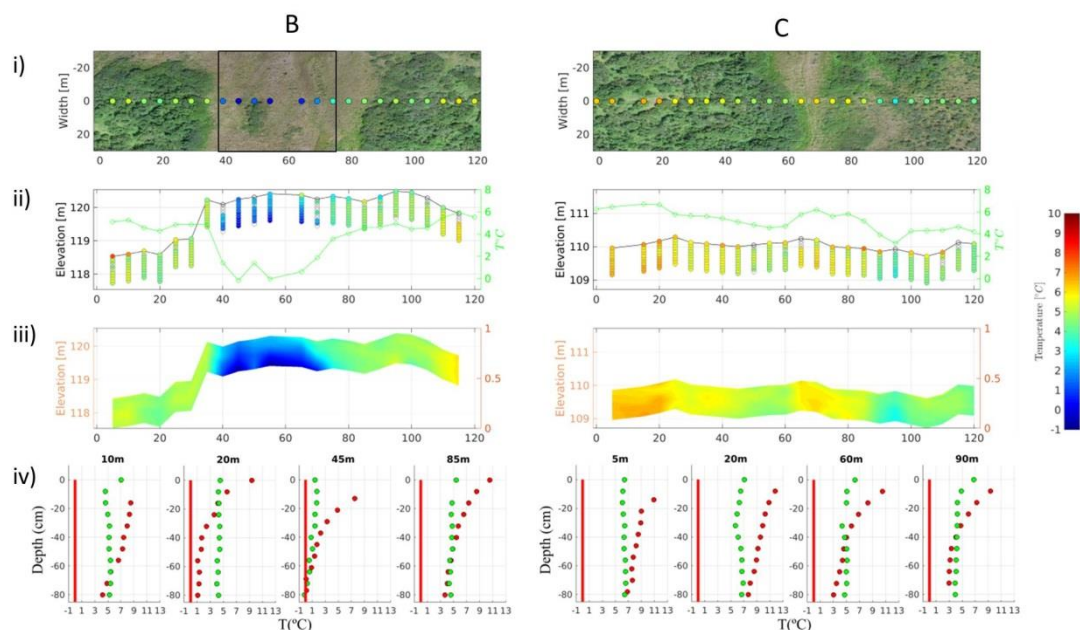


Figure 5: DTP data collected on September 20, 2017 along B and C transects. (i) Aerial view and identified shallow permafrost area (from Figure 3) overlain by soil temperature at 0.8 m depth, (ii) DTP temperature profiles and DTP temperature at 0.8 m depth, (iii) Interpolated temperature map of the first 0.8 meter with topography, and (iv) temperature profiles (green dots) at selected locations along the transects and compared to collocated temperature profiles acquired on July 17 (red dots, from Figure 3).

Figure 6i allows comparison of DTP data at 0.8 m depth with the ERT data acquired along the same transects at the same time on July 17, 2017. This comparison enables us to assess both the value and the limitations of the DTP system, and in particular to interpret the vertical extent of near-surface permafrost, based on shallow temperature measurements. The ERT transects indicate the presence of large and shallow resistive bodies (up to 10^4 Ohm.m, with highest resistivity values in the top 5 m) along transects A and B, which are quite isolated and have sharp lateral resistivity variations. Less resistive zones (approximately lower than 500 Ohm.m) surround these resistive bodies. The most conductive areas (around 300 Ohm.m) are located close to the surface and in some cases above the resistive bodies. Transects A and B exhibit the same type of resistivity distribution. Transects D and E have greater similarity to each other than to A and B, except for the shallow resistive area in the middle of transect E. Transect C has a conductive area positioned between deep resistive zones. The near-surface permafrost regions identified in the DTP data (temperatures that are at or below 0.2°C at 0.8 m depth) are collocated with the presence of shallow resistive bodies in the ERT data. This is the case between 15 and 75 m along transect A, 40 and 75 m along transect B, and 35 and 65 m along transect E. While thermo-petrophysical analysis of the ERT data is well beyond the scope of this study, here both the presence of resistive bodies in the ERT data and the collocated presence of low temperature values observed in the top 0.8 m confirm the presence of near-surface permafrost locations.

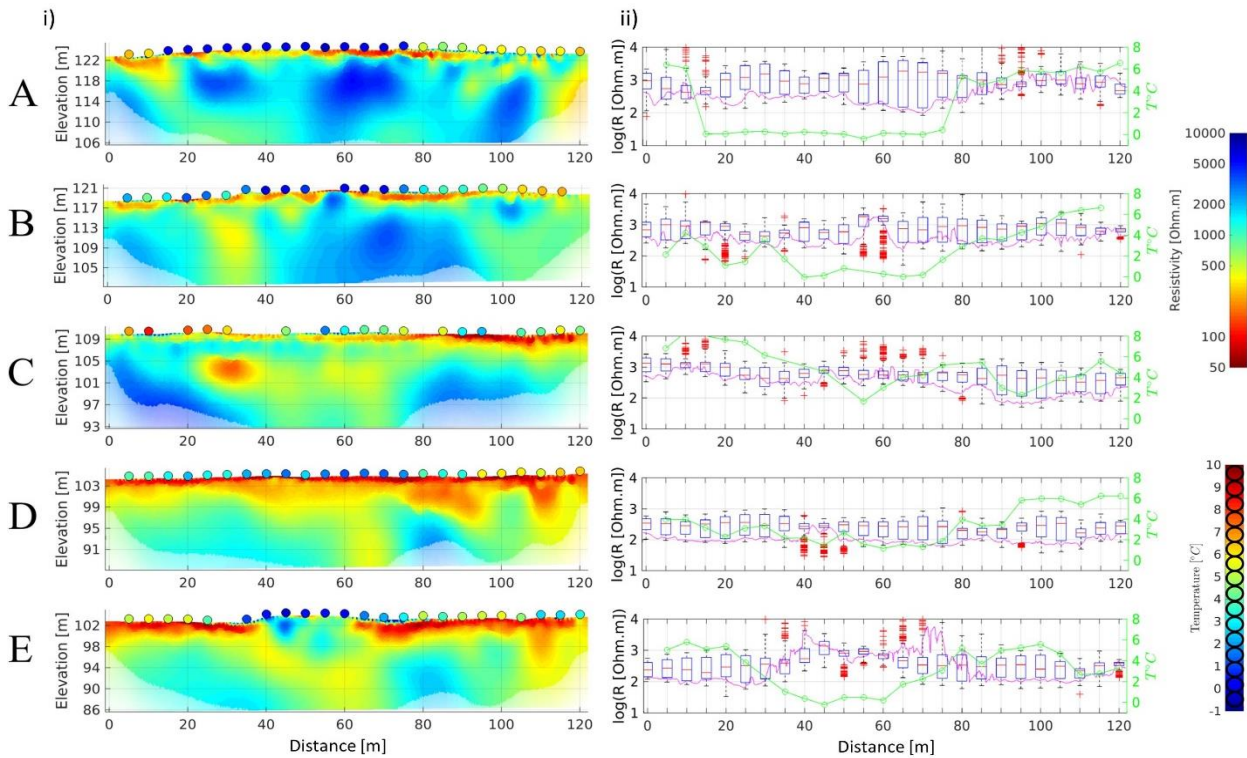


Figure 6: (i) ERT data with soil temperature at 0.8 m depth (extracted from the DTP dataset from July 17, 2017) shown at the top of each transect, and (ii) boxplots of the resistivity values in the top 7 m depth, vertically-averaged resistivity in the top 0.8 m (purple) and temperature at 0.8 m depth (green).

5 The DTP provides the temperature gradient in the top 0.8 m of soil, indicating the potential presence of permafrost at or deeper than this depth interval, while an increase in soil resistivity in the ERT is located where the ground is mostly frozen. Thus, both approaches provide different but complementary information about the depth of permafrost. Figure 6ii shows the DTP dataset at 0.8 m depth, the top 0.8 m depth average resistivity values for each DTP location, and the range of resistivity values (provided in a boxplot format) observed over the top 7 m depth in the ERT at each location. The top 0.8 m depth average resistivity value shows a spatial variability relatively similar to the soil-water-content data, with the exception of between 0 and 45 m along transect C. At shallow permafrost locations, the temperature profiles down to 0.8 m depth indicate temperature decreasing with depth toward the freezing point (generally located deeper than 0.8 m depth), while the ERT at similar depth is widely sensitive to the water content in the thawed layer. The DTP data at 0.8 m depth show more consistent co-variability with ERT data when considering the full range of resistivity values observed over the top 7 m in the ERT.

10



5 Discussion

In this section, we discuss the information contained in the DTP data and its potential, when coupled with other ground- and aerial-based geophysical datasets, for evaluating the distribution of permafrost.

5.1 Spatial Distribution of Near-Surface Permafrost

5 In environments where topography, soil water content, vegetation, snow thickness, soil-organic-matter content, and other parameters vary strongly over meters to tens of meters, understanding how these properties individually or in combination modulate the heat and water fluxes that influence permafrost distribution and temperature is very challenging. A key advantage of the DTP system is its ability to directly collect spatially dense (horizontal and vertical) soil temperature data. The DTP dataset discussed here provides information important to understanding the sub-Arctic ecosystem functioning at
10 the investigated site. First, it directly provides clear identification of near-surface permafrost locations, such as between 15 and 75 m along transect A, 40 and 75 m along transect B, and 35 and 65 m along transect E (Figure 3). The comparison between the main survey done on July 17 (Figure 3) and a second survey limited to transect B and C on September 20 (Figure 5) confirms the general spatial trend in soil temperature and identification of near-surface permafrost locations. The comparison also shows that the lateral extent of the permafrost body along transect B is a few meters smaller than initially
15 identified on July 17. It is clear that the identification of near-surface permafrost is less prone to uncertainty when performed at the end of the summer. Here, the observed variations along the sides of the near-surface permafrost also indicate the particularly complex spatiotemporal variability in lateral and vertical thermal fluxes occurring at these locations.

The DTP system also provides high-enough spatial resolution to observe possible relationships between soil temperature and topographic features, soil water content, and vegetation type. We find that in the study area near-surface permafrost
20 bodies are always located under topographic highs (at various scales), as seen in Figure 3. This co-variability is in agreement with the expectation that ground settlement will be limited in the presence of near-surface permafrost compared to surrounding locations with deeper or no permafrost. It is also consistent with the fact that topographic lows formed through ground settlement or erosion tend to have thicker snow cover during the winter, which provides more soil insulation and leads to warmer soil thermal conditions compared to topographically high regions (e.g., Wainwright et al., 2016).

25 Also, the presence of near-surface permafrost identified from the DTP dataset is strongly correlated with the presence of graminoids and/or lichens and dwarf-shrub-covered areas. The graminoid-dominated area crossing transect A (between 15 and 80 m) and B (between 40 and 80 m) can now be considered as encompassing a near-surface permafrost body (Figure 2). The lichen and dwarf-shrub region located along transect E (between 25 and 65 m) is also clearly identified and shows the lateral extent of the near-surface permafrost there.

30 Further, the soil moisture data suggests that the thaw layer above the near-surface permafrost bodies identified in transects A and B (and collocated with the presence of graminoids) is very wet if not fully saturated (Figure 3). We interpret this high-soil-water content in the thaw layer as associated with the limited drainage capacity imposed by the topography and



the presence of near-surface permafrost. Given the thermal properties of water, one could expect to observe thicker soil thaw layer where soil is fully water saturated compared to dry soil (Tran et al., 2017). This relationship is clear when comparing the very shallow thaw layer above permafrost (~0.45 m depth) observed at 45 m along transect E to the area with deeper thaw layer along transects A and B. Indeed, the driest soil is observed at 45 m along transect E (Figure 3). While this relation is observed between these two locations where near-surface permafrost is present, the soil water content in the thaw layer above the shallow permafrost along transects A and B is higher than at many other locations where no shallow permafrost is present. The influence of soil water content on thermal parameters and regime is certain but complex, because of water phase changes and soil water content temporal variability controlled by hydraulic parameter and thermal hydrology.

DTP measurements and related identification of near-surface permafrost locations is consistent with ERT data, where high resistivity bodies are identified at similar locations along the transects and at shallow depth (Figure 6). The high resistivity values observed in the shallow depth (top 4 m) in the ERT are generally located deeper than where the 0°C is expected from the DTP data. This is not unexpected: it can result from (i) smoothness in the ERT inversion, (ii) the presence of still large unfrozen water content at temperatures between -2 and 0°C, and/or (iii) particularly large unfrozen water content during freezing where the total water content is high.

The combination of DTP data and ERT is also valuable for investigating the subsurface vertical heterogeneity in regions where near-surface permafrost bodies are present. The identified near-surface permafrost bodies extend vertically to about 15 m depth along transects A and B, but much less along transect E, based on the ERT data (Figure 6). Assuming constant salinity and homogeneous lithology, the ERT suggests that the coldest and most strongly frozen regions of near-surface permafrost bodies occur at depths of about 6 m along transects A and B, and at about 2 m depth along transect E. The DTP data and thaw layer thickness indicate shallowest top of permafrost along transect E, which is consistent with the ERT data. While temperature in the DTP data could be valuable by itself, adding the ERT in this case enables us to clearly identify locations where near-surface permafrost is thin.

5.2 Beyond the Identification of Near-Surface Permafrost Locations

While the value and promise of the DTP system for improving our understanding of near-surface permafrost distribution and related shallow lateral and vertical variation in temperature regimes have been demonstrated in the previous section, the variations in soil temperature, where deep permafrost—with a perennially thawed zone above it—or no permafrost is present, are more difficult to interpret.

When surface water content is high and the permafrost table is deep or permafrost is absent, the thermal profile shows relatively low temperatures right below the surface, with a relatively small vertical temperature gradient. This is the case between 0 and 70 m along transect D and between 0 and 30 and 65 and 120 m along transect E (Figure 3). These locations are at the flat toe of the hillslope, with the groundwater table at or very close to the surface. The soil temperature at these locations is around 1-2°C at 0.80 m depth, and possibly decreases below 0°C at much greater depths. We interpret the large soil water content and some water inundation to be maintaining a relatively homogeneous and stable shallow temperature



regime, owing to the water's high heat capacity. In such a wet environment, the latent heat effect is likely reinforced as well. The melting pore ice can absorb additional heat and slow the rate of temperature increase. Similarly, as temperature decreases in autumn, freezing pore water releases latent heat and slows temperature decline (Osterkamp and Romanovsky, 1997; Shojae Ghias et al., 2017). At such locations, the DTP data indicate that a perennially thawed zone may be present, along with the possible presence of deeper permafrost.

Another interesting case is along transect C (Figure 3) between 0 and 30 m. At this location, the DTP data show a very small thermal gradient between the surface and 0.8 m depth, where the temperature is still as high as $\sim 7^{\circ}\text{C}$. In addition, this location has a ground elevation that is slightly higher than the rest of the transect, is relatively dry at the surface, is situated in tall shrub area where snow depth may be large during the winter, and is interpreted to have some rocky soil based on probe installation. This relatively dry and rocky location suggests that the soil in this region has a low heat capacity, which would decrease the ability of soil to maintain its temperature in the surveyed depth interval and produce a small thermal gradient as observed here. This is confirmed by the September 20 DTP data between 0 and 30 m along transect C (Figure 5iv) showing colder soil temperatures in the entire 0-0.8 m surveyed depth interval (compared to July 17), which indicates that the colder air temperature in September likely had already a strong influence on the entire temperature profile. This is different from most of the other locations, which show an increase in soil temperature at 0.8 m depth between July 17 and September 20. In addition to dry and rocky material that could explain the limited ability of soil to maintain its temperature in the surveyed depth interval, a change in soil thermal parameters below the surveyed depth interval may further impede the transfer of heat to a deeper layer. At this time, we cannot confirm if the deeper layer, which indeed is resistive in the ERT data, were permafrost or bedrock. The end of transects A and B most likely exhibit the same physical process discussed above, in which shallow temperature is relatively warm and water content relatively low, producing higher uncertainty regarding permafrost presence at depths greater than 4 m.

The aforementioned results, and the complexity involved in how temperature flux is modulated by various surface properties and soil heterogeneity, underscore the importance of surveying numerous locations, and measuring soil temperature profiles down to 0.8 m depth or deeper, ideally over time. The DTP system and the long-term monitoring stations 2 and 9 show that measuring just the very-shallow surface temperature (first 30 cm) is insufficient to evaluate deeper thermal regimes (Figure 4). Temporal variations in soil temperature in the top 10 to top 30 cm can be significant over short periods of time (up to hour scale), and not representative of deeper thermal regimes, especially in dry areas. In addition, the strong decay in temperature in the top 30 cm can produce larger error within temperature data, in case of uncertainty as to the exact depth where the point sensor is located. This expected behavior, based on the physics of thermal flux, confirms the need for measuring temperature with high vertical resolution close to the surface as well as at depths deeper than 0.5 m, where asymptotic trends in soil temperature at depth are more present. In addition, the comparison of July 17 and September 20 surveys (Figure 5) shows that observing the system over time provides, as expected, very valuable information to go beyond the identification of near-surface permafrost. The DTP dataset will clearly benefit from year-round acquisition of soil temperature measurements at different depths, which are key for the interpretation of both surface energy balance and deeper



thermal characteristics and regimes. High vertical resolution close to the surface (Figure 3) has the potential to provide information on freezing or thawing fronts in shoulder seasons, as well as on the influence of organic layers on deeper thermal regimes.

Finally, based on the long-term monitoring station data (Figure 4), we expect that obtaining the fluctuation in temperature over time using the DTS will improve the ability to evaluate various regimes and factors. We also expect the time-lapse soil measurements to be useful as input to inverse modeling techniques focused on estimating soil thermal parameters and possibly soil-organic-matter content (e.g., Nicolsky et al., 2009; Tran et al., 2017).

6 Conclusion

This study describes and tests a novel strategy referred to as Distributed Temperature Profiling (DTP) to quantify the near-surface soil-thermal state at an unprecedented number of depths and locations. To our knowledge, this is the first time that a thermal characterization approach has provided such high vertical and lateral density in measurements. The low cost, portability, and ease of deploying the DTP system makes this method efficient for investigating permafrost spatial heterogeneity, particularly at discontinuous permafrost sites such as investigated in this study (where significant lateral variations in soil temperature occur over meters to tens of meters). As shown, the densely spaced DTP data compared well with classical thermal measurements and provided much higher spatial resolution. Possible deployment of DTP systems in a time-lapse mode will also enable high temporal resolution and larger temporal coverage.

In this study, the DTP dataset has shown to be particularly valuable in delineating the presence of near-surface permafrost. When combined with other approaches, the DTP was also useful for evaluating correspondences between summer soil temperature, plant type, topography, soil water content, and deeper subsurface structure. While decoupling the control of these and other factors (e.g., organic content and snow depth) on thaw layer thickness and the depth of permafrost table is complex and beyond the scope of this paper, our data suggest that changes in soil temperatures often correspond to changes in topography, vegetation, and soil moisture. Near-surface permafrost identified in the study area using the DTP data is primarily collocated under topographic highs and under areas covered with graminoids or lichens and dwarf shrubs. The results provide new insights about the presence or absence of near-surface permafrost bodies.

The simple and low-cost DTP strategy holds promise for improving our ability to quantify local permafrost distribution and to explore interactions between complex Arctic ecosystem properties and processes. In particular, coupling various observations has the potential to advance strategies to estimate permafrost distribution from remotely sensed information, including topography, vegetation, and possibly surficial moisture characteristics. This study opens the door to such quantification, although many challenges remain. For example, while co-variability is observed between near-surface permafrost and topographic highs, delineating near-surface permafrost bodies in such an environment through automated extraction of topographic highs at various scales—while removing the larger-scale topographic trend—is still difficult. Similarly, identifying physical characteristics of tall shrub patches from remote sensing data is still challenging.



Ongoing developments in the DTP system include the miniaturization and cost-reduction of the data-logger, improvement and cost-reduction of the temperature probe fabrication, ability to produce probes with variable length and vertical resolution, development of open-source software and hardware to encourage community-based development and deployment, and automated acquisition and data transfer for long-term monitoring purposes. These developments will enable the deployment of low-cost DTP to measure and record ground temperatures all year-round and with a number of probes that are well beyond that described in this study. The potential of this method for characterizing and monitoring a variety of near-surface heat and related water dynamic processes is significant for informing investigations aimed at quantifying water infiltration, evaporation, biogeochemical processes, hyporheic exchange, snow-melt dynamics, and permafrost evolution.

Acknowledgments

We acknowledge the assistance of Todd Wood, Paul Cook, and Alejandro Morales of the Geoscience Measurement Facility (GMF, gmf.lbl.gov) at LBNL for building the DTP system. The probe sleeve and filling material were partly influenced by the work of Bill Cable (UAF, AK). Datasets are available upon request by contacting the corresponding author. The Next-Generation Ecosystem Experiments (NGEE-Arctic) project is supported by the Office of Biological and Environmental Research in the DOE Office of Science. This NGEE-Arctic research is supported through contract number DE-AC02-05CH11231 to Lawrence Berkeley National Laboratory.

References

- Ashton, K.: That "Internet of Things" thing, *J. RFID*, 168, 2009.
- Binley, A. and Kemna, A.: DC Resistivity and Induced Polarization Methods. In: *Hydrogeophysics*, Rubin, Y. and Hubbard, S. S. (Eds.), Springer Netherlands, 2005.
- Biskaborn, B. K., Lanckman, J. P., Lantuit, H., Elger, K., Streletskiy, D. A., Cable, W. L., and Romanovsky, V. E.: The new database of the Global Terrestrial Network for Permafrost (GTN-P), *Earth System Science Data*, 7, 245-259, 2015.
- Brewer, M. C.: The thermal regime of an Arctic lake, *Eos, Transactions American Geophysical Union*, 39, 278-284, 1958.
- Briggs, M. A., Lautz, L. K., McKenzie, J. M., Gordon, R. P., and Hare, D. K.: Using high-resolution distributed temperature sensing to quantify spatial and temporal variability in vertical hyporheic flux, *Water Resources Research*, 48, 2012.
- Burn, C. R.: Tundra lakes and permafrost, Richards Island, western Arctic coast, Canada, *Canadian Journal of Earth Sciences*, 39, 1281-1298, 2002.
- Cable, W. L., Romanovsky, V. E., and Jorgenson, M. T.: Scaling-up permafrost thermal measurements in western Alaska using an ecotype approach, *The Cryosphere*, 10, 2517-2532, 2016.



- Dafflon, B., Hubbard, S., Ulrich, C., Peterson, J., Wu, Y., Wainwright, H., and Kneafsey, T. J.: Geophysical estimation of shallow permafrost distribution and properties in an ice-wedge polygon-dominated Arctic tundra region, *GEOPHYSICS*, 81, WA247-WA263, 2016.
- Dafflon, B., Oktem, R., Peterson, J., Ulrich, C., Tran, A. P., Romanovsky, V., and Hubbard, S. S.: Coincident aboveground and belowground autonomous monitoring to quantify covariability in permafrost, soil, and vegetation properties in Arctic tundra, *Journal of Geophysical Research: Biogeosciences*, 122, 1321-1342, 2017.
- Davesne, G., Fortier, D., Domine, F., and Gray, J. T.: Wind-driven snow conditions control the occurrence of contemporary marginal mountain permafrost in the Chic-Choc Mountains, south-eastern Canada: a case study from Mont Jacques-Cartier, *The Cryosphere*, 11, 1351-1370, 2017.
- Davidson, E. A. and Janssens, I. A.: Temperature sensitivity of soil carbon decomposition and feedbacks to climate change, *Nature*, 440, 165-173, 2006.
- Dougherty, D.: The maker movement, *Innovations*, 7, 11-14, 2012.
- Fang, C. and Moncrieff, J. B.: The dependence of soil CO₂ efflux on temperature, *Soil Biology & Biochemistry*, 33, 155-165, 2001.
- Gisnås, K., Westermann, S., Schuler, T. V., Litherland, T., Isaksen, K., Boike, J., and Etzelmüller, B.: A statistical approach to represent small-scale variability of permafrost temperatures due to snow cover, *The Cryosphere*, 8, 2063-2074, 2014.
- Gubler, S., Fiddes, J., Keller, M., and Gruber, S.: Scale-dependent measurement and analysis of ground surface temperature variability in alpine terrain, *The Cryosphere*, 5, 431-443, 2011.
- Hauck, C.: Frozen ground monitoring using DC resistivity tomography, *Geophysical Research Letters*, 29, 12-11-12-14, 2002.
- Hausner, M. B., Suarez, F., Glander, K. E., van de Giesen, N., Selker, J. S., and Tyler, S. W.: Calibrating Single-Ended Fiber-Optic Raman Spectra Distributed Temperature Sensing Data, *Sensors*, 11, 10859-10879, 2011.
- Hilbich, C., Hauck, C., Hoelzle, M., Scherler, M., Schudel, L., Völksch, I., Mühll, D. V., and Mäusbacher, R.: Monitoring mountain permafrost evolution using electrical resistivity tomography: A 7--year study of seasonal, annual, and long--term variations at Schilthorn, Swiss Alps, *Journal of Geophysical Research: Earth Surface*, 113, 2008.
- Holden, Z. A., Swanson, A., Klene, A. E., Abatzoglou, J. T., Dobrowski, S. Z., Cushman, S. A., Squires, J., Moisen, G. G., and Oyler, J. W.: Development of high-resolution (250 m) historical daily gridded air temperature data using reanalysis and distributed sensor networks for the US Northern Rocky Mountains, *International Journal of Climatology*, 36, 3620-3632, 2016.
- Hubbard, S. S., Gangodagamage, C., Dafflon, B., Wainwright, H., Peterson, J., Gusmeroli, A., Ulrich, C., Wu, Y., Wilson, C., Rowland, J., and others: Quantifying and relating land-surface and subsurface variability in permafrost environments using LiDAR and surface geophysical datasets, *Hydrogeology Journal*, 21, 149-169, 2013.
- Hubbart, J., Link, T., Campbell, C., and Cobos, D.: Evaluation of a low-cost temperature measurement system for environmental applications, *Hydrological Processes*, 19, 1517-1523, 2005.



- Jafarov, E., Coon, D. T., Harp, D. R., Wilson, C. J., Painter, S. L., Atchley, A. L., and Romanovsky, V. E.: Modeling the role of preferential snow accumulation in through talik development and hillslope groundwater flow in a transitional permafrost landscape, *Environmental Research Letters*, 13, 105006, 2018.
- Jorgenson, M. T., Romanovsky, V., Harden, J., Shur, Y., O'Donnell, J., Schuur, E. A. G., Kanevskiy, M., and Marchenko, S.:
5 Resilience and vulnerability of permafrost to climate change, *Canadian Journal of Forest Research*, 40, 1219-1236, 2010.
- Krautblatter, M., Verleysdonk, S., Flores-Orozco, A., and Kemna, A.: Temperature-calibrated imaging of seasonal changes in permafrost rock walls by quantitative electrical resistivity tomography (Zugspitze, German/Austrian Alps), *Journal of Geophysical Research: Earth Surface*, 115, 2010.
- Lachenbruch, A. and Marshall, B.: Heat Flow in the Arctic, *ARCTIC*, 22, 300-311, 1969.
- 10 Léger, E., Dafflon, B., Soom, F., Peterson, J., Ulrich, C., and Hubbard, S.: Quantification of Arctic Soil and Permafrost Properties Using Ground-Penetrating Radar and Electrical Resistivity Tomography Datasets, *IEEE Journal of Selected Topics in Applied Earth Observations and Remote Sensing*, 10, 4348-4359, 2017.
- Lewkowicz, A. G., Bonnaventure, P. P., Smith, S. L., and Kuntz, Z.: Spatial and thermal characteristics of mountain permafrost, northwest canada, *Geografiska Annaler: Series A, Physical Geography*, 94, 195-213, 2012.
- 15 Lundquist, J. D. and Lott, F.: Using inexpensive temperature sensors to monitor the duration and heterogeneity of snow-covered areas, *Water Resources Research*, 44, 2008.
- Marescot, L., Monnet, R. e., gis, and Chapellier, D.: Resistivity and induced polarization surveys for slope instability studies in the Swiss Alps, *Engineering Geology*, 98, 18-28, 2008.
- Minsley, B. J., Abraham, J. D., Smith, B. D., Cannia, J. C., Voss, C. I., Jorgenson, M. T., Walvoord, M. A., Wylie, B. K.,
20 Anderson, L., Ball, L. B., Deszcz-Pan, M., Wellman, T. P., and Ager, T. A.: Airborne electromagnetic imaging of discontinuous permafrost, *Geophysical Research Letters*, 39, 2012.
- Nicolisky, D. J., Romanovsky, V. E., and Panteleev, G. G.: Estimation of soil thermal properties using in-situ temperature measurements in the active layer and permafrost, *Cold Regions Science and Technology*, 55, 120-129, 2009.
- Osterkamp, T. E.: Freezing and thawing of soils and permafrost containing unfrozen water or brine, *Water Resources*
25 *Research*, 23, 2279-2285, 1987.
- Osterkamp, T. E.: Response of Alaskan permafrost to climate, *Proceedings of the Fourth International Conference on Permafrost*, Fairbanks, 1983, 145-152.
- Osterkamp, T. E.: Temperature measurement in Permafrost, *Alaska DOTPF*, Fairbanks, AK, 87 pp., 1985.
- Osterkamp, T. E. and Gosink, J. P.: Variations in permafrost thickness in response to changes in paleoclimate, *Journal of*
30 *Geophysical Research: Solid Earth*, 96, 4423-4434, 1991.
- Osterkamp, T. E. and Romanovsky, V. E.: Freezing of the Active Layer on the Coastal Plain of the Alaskan Arctic, *Permafrost and Periglacial Processes*, 8, 23-44, 1997.



- Roger, J., Allard, M., Sarrazin, D., L'Hérault, E., Doré, G., and Guimond, A.: Evaluating the use of distributed temperature sensing for permafrost monitoring in Salluit, Nunavik, 68th Canadian geotechnical conference and 7th Canadian permafrost conference; GEOQuébec 2015, Vancouver, BC, Canada, 2015.
- Romanovsky, V. E. and Osterkamp, T. E.: Effects of unfrozen water on heat and mass transport processes in the active layer and permafrost, *Permafrost and Periglacial Processes*, 11, 219-239, 2000.
- Romanovsky, V. E. and Osterkamp, T. E.: Interannual variations of the thermal regime of the active layer and near-surface permafrost in northern Alaska, *Permafrost and Periglacial Processes*, 6, 313-335, 1995.
- Rowland, J. C., Travis, B. J., and Wilson, C. J.: The role of advective heat transport in talik development beneath lakes and ponds in discontinuous permafrost, *Geophysical Research Letters*, 38, 2011.
- 10 Rucker, C., Günther, T., and Spitzer, K.: 3-d modeling and inversion of DC resistivity data incorporating topography - Part I: Modeling, *Geophysical Journal International*, 166, 495-505, 2006.
- Rucker, C., Günther, T., and Wagner, F. M.: pyGIMLi: An open-source library for modelling and inversion in geophysics, *Computers & Geosciences*, 109, 106 - 123, 2017.
- Rucker, T. G. C. and Spitzer, K.: 3-d modeling and inversion of DC resistivity data incorporating topography - Part II: Inversion, *Geophysical Journal International*, 166, 506-517, 2006.
- 15 Schön, J. H.: *Physical properties of rocks: Fundamentals and principles of petrophysics*, Elsevier, 2015.
- Shojae Ghias, M., Therrien, R., Molson, J., and Lemieux, J.-M.: Controls on permafrost thaw in a coupled groundwater-flow and heat-transport system: Iqaluit Airport, Nunavut, Canada, *Hydrogeology Journal*, 25, 657-673, 2017.
- Smits, K. M., Cihan, A., Sakaki, T., and Illangasekare, T. H.: Evaporation from soils under thermal boundary conditions: Experimental and modeling investigation to compare equilibrium- and nonequilibrium-based approaches, *Water Resources Research*, 47, 2011.
- 20 Stieglitz, M., Dèry, S. J., Romanovsky, V. E., and Osterkamp, T. E.: The role of snow cover in the warming of arctic permafrost, *Geophysical Research Letters*, 30, 2003.
- Stonestrom, D. A. and Constantz, J. (Eds.): *Heat as a tool for studying the movement of ground water near streams*, U.S. Geol. Surv. Circ, 2003.
- 25 Sturm, M., Racine, C., and Tape, K.: Increasing shrub abundance in the Arctic, *Nature*, 411, 546, 2001.
- Swartz, J. H.: A geothermal measuring circuit, *Science*, 120, 573-574, 1954.
- Tran, A. P., Dafflon, B., and Hubbard, S. S.: Coupled land surface--subsurface hydrogeophysical inverse modeling to estimate soil organic carbon content and explore associated hydrological and thermal dynamics in the Arctic tundra, *The Cryosphere*, 11, 2089-2109, 2017.
- 30 Tyler, S. W., Selker, J. S., Hausner, M. B., Hatch, C. E., Torgersen, T., Thodal, C. E., and Schladow, S. G.: Environmental temperature sensing using Raman spectra DTS fiber-optic methods, *Water Resources Research*, 45, 2009.



- Wagner, A. M., Lindsey, N. J., Dou, S., Gelvin, A., Saari, S., Williams, C., Ekblaw, I., Ulrich, C., Borglin, S., Morales, A., and Ajo-Franklin, J.: Permafrost Degradation and Subsidence Observations during a Controlled Warming Experiment, *Scientific Reports*, 8, 2018.
- Wainwright, H. M., Dafflon, B., Smith, L. J., Hahn, M. S., Curtis, J. B., Wu, Y., Ulrich, C., Peterson, J. E., Torn, M. S., and
5 Hubbard, S. S.: Identifying multiscale zonation and assessing the relative importance of polygon geomorphology on carbon fluxes in an Arctic tundra ecosystem, *Journal of Geophysical Research: Biogeosciences*, 120, 788-808, 2015.
- Wainwright, H. M., Liljedahl, A. K., Dafflon, B., Ulrich, C., Peterson, J. E., and Hubbard, S. S.: Mapping snow depth within a tundra ecosystem using multiscale observations and Bayesian methods, *Cryosphere*, 168, 2016.
- Whiteman, C. D., Hubbe, J. M., and Shaw, W. J.: Evaluation of an inexpensive temperature datalogger for meteorological
10 applications, *Journal of Atmospheric and Oceanic Technology*, 17, 77-81, 2000.
- Wu, Y., Hubbard, S. S., Ulrich, C., and Wulschleger, S. D.: Remote monitoring of freeze--thaw transitions in Arctic soils using the complex resistivity method, *Vadose Zone Journal*, 12, 2013.
- Yoshikawa, K. and Hinzman, L. D.: Shrinking thermokarst ponds and groundwater dynamics in discontinuous permafrost near Council, Alaska, *Permafrost and Periglacial Processes*, 14, 151-160, 2003.
- 15 Zhang, T.: Influence of the seasonal snow cover on the ground thermal regime: An overview, *Reviews of Geophysics*, 43, 2005.
- Zhang, T., Osterkamp, T. E., and Stamnes, K.: Some Characteristics of the Climate in Northern Alaska, U.S.A, *Arctic and Alpine Research*, 28, 509-518, 1996.